King Saud University

Arabian Journal of Chemistry

ORIGINAL ARTICLE

Influence of oxygen functionalization on physico-chemical properties of imidazolium based ionic liquids – Experimental and computational study

Aleksandar Tot [a], Črtomir Podlipnik [b], Marija Bešter-Rogač [b], Slobodan Gadžurić [a], Milan Vraneš [a],[*]

[a] *University of Novi Sad, Faculty of Sciences, Department of Chemistry, Biochemistry and Environmental Protection, Trg D. Obradovića 3, 21000 Novi Sad, Serbia*
[b] *Faculty of Chemistry and Chemical Technology, University of Ljubljana, Večna pot 113, 1000 Ljubljana, Slovenia*

Abstract In this work, four different oxygen functionalized ionic liquids, 1-(3-hydroxypropyl)-3-methylimidazolium chloride,[OHC$_3$mIm][Cl], 1-(3-hydroxypropyl)-3-ethylimidazolium chloride [OHC$_3$eIm][Cl], 1-(2-oxobutyl)-3-methylimidazolium chloride, [C$_2$OC$_2$mIm][Cl] and 1-(4-hydroxy-2-oxobutyl)-3-methylimidazolium chloride, [OHC$_2$OC$_2$mIm][Cl] were synthesized in liquid state at room temperature. Detailed physico-chemical characterisation (density, viscosity and conductivity) supported with computational simulations for pure ionic liquid and their aqueous solutions were performed. Based on these examinations, interactions in pure ionic liquids and interactions between water and synthesized ionic liquids were discussed.

© 2017 Production and hosting by Elsevier B.V. on behalf of King Saud University. This is an open access article under the CC BY-NC-ND license (http://creativecommons.org/licenses/by-nc-nd/4.0/).

1. Introduction

One of the attractive attributes of ILs is the potential to generate a wide range of types of ILs with fine-tuned physico-chemical properties by the combination of various cations with anions, along with rational functionalization of ions (Neale et al. 2017, Coadou et al. 2016, Deng et al.,2011; Tang et al., 2012; Fei et al., 2006; Liu et al., 2005). The idea of task-specific ionic liquids (TSILs) carrying specific functionality tailored for certain applications has become more popular, and an impressive catalog of TSILs with pendant acid, base, alcohol, or ether groups on one (or both) of the ions are recently synthesized (Kuhlmann et al. 2007; Yue et al., 2011). Of historical relevance, poly(ethylene oxide)s (PEOs) (also known as poly(ethylene glycol)s, PEGs) have been incorporated into cationic (or anionic) units to yield the liquid state of ion conductive polymers (Ohno, 2006; Yoshizawa and Ohno, 2001). There is a rising interest in functionalizing ILs by adding ether or hydroxyl groups to IL cations based on different ions, including imidazolium (Ohno, 2006; Yoshizawa and Ohno,

Production and hosting by Elsevier

2001; Pernak et al., 2001; Branco et al., 2002; Domanska and Marciniak, 2005; Wang et al., 2007), pyridinium (Pernak and Branicka, 2003), quaternary ammonium (Matsumoto et al., 2005), phosphonium (Tsunashima and Sugiya, 2007), piperidinium (Zhou et al., 2006), pyrrolidinium (Zhou et al., 2006), guanidinium (Fang et al., 2009), sulfonium (Han et al., 2010), oxazolidinium (Zhou et al., 2006) and morpholinium types (Zhou et al., 2006). In a short period, these functionalized ILs have shown attractive physico-chemical properties and applications in several exciting areas (Seddon, 1997; Welton, 1999; Hallett and Welton 2011; van Rantwijk and Sheldon, 2007; Yang and Pan, 2005; Zhao, 2010; Moniruzzaman et al., 2010; Fan et al., 2017; Fareghi-Almadari et al., 2017).

ILs with oxygen (hydroxyl and/or ether) functionalized cations, which was first reported by Branco et al. (2002) provide classical ILs with useful polarity/solvation properties, and could replace traditional alcohols in certain applications. Oxygen functionalized ILs was found to play an important role on the enzymatic reactions, to enhance the enzyme activity and increase the enantioselectivity (Tang et al., 2012; Dreyer and Kragl, 2008). Hydroxyl and/or ether functionalized ILs were also suggested as excellent stabilizer for the synthesis of nanostructure material (Choi et al., 2007; Hou et al., 2007). Also, hydroxyl ILs-based chloro- Ni(II) complexes were found to show effective thermochromic behaviour with wider temperatures and more stable repeated operations, wherein the hydroxyl group in ILs is more effective than those in water and alcohols to coordinate with the metal ion in the octahedral configuration (Wei et al.,2008). However, despite their extensive application of oxygen functionalized ILs and the large number of studies published in the past few years, some of their unique properties remain poorly understood, and little has been conducted to explore the relationship between ILs structure and they properties.

Also, ionic liquid, 1-(2-hydroxy)ethyl-3-methylimidazolium chloride was already synthesized, and it is found to be in solid state at room temperature (Yokozeki and Shiflett, 2010; Nie et al., 2012; Vraneš et al., 2016). Following the rules for other imidazolium ionic liquids, it was expected that prolongation of alkyl chain will increase melting point (Xue et al., 2016). Suprisingly, 1-(3-hydroxy)propyl-3-methylimidazolium chloride, synthesized in this work was liquid at room temperature, as well as three additional oxygen functionalized imidazolium chloride ionic liquids. According to this, detailed physico-chemical characterisation (density, viscosity and conductivity measurements), supported with molecular simulations was obtained for pure ionic liquids and their aqueous solutions, in order to explain why this ionic liquids are liquid at room temperature and how oxygen functionalization impact on interactions with water.

2. Experimental and mathematical approach

2.1. Synthesis

All chemicals for ILs synthesis were used without purification as purchased from the manufacturer: 1-methylimidazole (Sigma Aldrich, CAS number: 616-47-7, $\omega \geq 0.99$), 1-ethylimidazole (Merck, CAS number: 7098-07-9, $\omega \geq 0.98$); 2-chloroethyl ethyl ether (Sigma Aldrich, CAS number:

628-34-2, $\omega \geq 0.99$), 3-chloro-1-propanol (Sigma Aldrich, CAS number: 627-30-5, $\omega \geq 0.98$), 2-(2-chloroethoxy)ethanol (Sigma Aldrich, CAS number: 628-89-7, $\omega \geq 0.99$), ethyl acetate (Sigma Aldrich, CAS number: 141-78-6, $\omega \geq 0.998$).

3-chloro-1-propanol (or 2-(2-chloroetoxy)ethanol or 2-chloroethyl ethyl ether) and 1-methylimidazole (or 1-ethylimidazole) were added to a round-bottom flask. Ethyl acetate was used as a solvent, and 3-chloro-1-propanol (or 2-(2-chloroetoxy)ethanol or 2-chloroethyl ether) was added in 10% excess. The mixture was kept under the reflux for 48 h at 70 °C with stirring and two phases were formed. The top phase, containing unreacted starting material was removed. The bottom phase was washed four times with new portion of ethyl acetate. The products were obtained in the liquid state, and additionally was dried under vacuum with P_2O_5 for the next 72 h. Water content in synthesized ionic liquids are determined by Karl-Fisher titration and results are presented in Table S1.

For the newly synthesized ionic liquids, nuclear magnetic resonance (NMR) data were recorded in $CDCl_3$ at 298.15 K on a Bruker 300 DRX spectrometer (Coventry, UK) and the solvent peak was used as reference. Infrared spectra were recorded as neat samples from 4000 to 650 cm^{-1} on a Thermo-Nicolet Nexus 670 spectrometer fitted with a Universal ATR Sampling Accessory. Obtained NMR and IR spectra with adequate assignation are given in Supporting information in Figs. S1–S8.

2.2. Density measurements

2.2.1. Pure ionic liquids

The vibrating tube Rudolph Research Analytical DDM 2911 densimeter with the accuracy and precision of ± 0.00001 g cm^{-3} was used for density measurements. The instrument was thermostated (Peltier-type) within ± 0.01 K and viscosity was automatically corrected. Before each series of measurements calibration of the instrument was performed at the atmospheric pressure. The calibration procedure is described in our previous papers (Vraneš et al., 2016). Each experimental density value is the average of at least three measurements at temperatures from (293.15 to 313.15) K. Repeated experimental measurements showed reproducibility within 0.01%, and an average value is presented in this work. Standard uncertainty of determining the density is less than $4.9 \cdot 10^{-4}$ g cm^{-3}.

2.2.2. Aqueous solutions

The binary mixtures (ILs + water) were measured at atmospheric pressure of 0.1 MPa using a vibrating tube Anton Paar DMA 5000 densimeter with a declared reproducibility of $1 \cdot 10^{-3}$ kg m^{-3}. Before each series of measurements calibration of the instrument was performed at the atmospheric pressure using triple distilled ultra pure water in the temperature range from (278.15 to 313.15) K. The instrument was thermostated within ± 0.001 K and viscosity related errors in the density were automatically corrected over full viscosity range. To avoid gas bubbles entrapped in the measuring cell filled with a sample, the cell was filled carefully to minimize the probability of such error. The total volume of the sample used for density measurements was approximately 1 cm^3. Densimeter already has incorporated moisture adsorbent. The relative

standard uncertainty of determining the density was estimated to be $3.15 \cdot 10^{-4}$ g cm^{-3}.

From the experimental densities the apparent molar volumes, V_Φ, partial molar volumes of water and ILs were calculated using the procedure described elsewhere (Vraneš et al., 2016). The results are tabulated in Table S2.

2.3. Viscosity measurements

The viscosities of the solutions were determined with a micro Ubbelohde viscometers (SI Analytics GmbH, Mainz, Germany, type No. 526 10 capillary I and type No. 526 20 capillary II) and an automatic flow time measuring system ViscoSystem® AVS 370. The viscometer was immersed in a transparent thermostat bath where the temperature was maintained from (293.15 to 313.15) ± 0.01 K. Each measurement was automatically repeated at least five times and yielded a reproducibility of the flow time of < 0.02%. The kinematic viscosity of solutions, v(m^2 s^{-1}), was calculated from the equation $v = Ct\text{-}E/t$, where t (s) is the flow time, $C = 1.00669 \cdot 10^{-8}$ m^2 s^{-2} and $E = 1.3785 \cdot 10^{-5}$ m^2 s are constants characteristic for the viscometer and were determined by calibration of the viscometer with water at 293.15 and 298.15 K. The absolute (dynamic) viscosity, η was obtained from the relation $\eta = v \cdot \rho$, where ρ is density of the investigated solution and results are presented in Table S3. The errors from calibration and temperature control yielded an uncertainty less than 0.05% of absolute viscosity.

2.4. Electrical conductivity measurements

2.4.1. Pure ionic liquids

Electrical conductivity measurements of pure ILs were carried out in a Pyrex-cell with platinum electrodes in the temperature range (293.15 to 313.15) K on a conductivity meter Jenco 3107 using DC signal. The cell constant amounted to 1.0353 cm^{-1} was checked from time to time to control any possible evolution. The relative standard uncertainty for electrical conductivity was less than 1.5%. All obtained experimental values represent the mean of three measurements.

2.4.2. Aqueous solutions

Conductivity measurements were performed with a three electrode flow cell connected to a mixing chamber and mounted underneath a lid suitable for immersion in a thermostat bath. The cell was calibrated with aqueous potassium chloride solutions following procedure of Barthel et al. (1980) The computer – controlled measurement system, based on a high-precision thermostat (Lauda UB40J, WK 1400) and an impedance analyzer (Agilent 4284A) was described in detail previously. (Bešter-Rogač et al., 2011) The system allows automatic setting of each temperature of the measurement program with reproducibility better than 0.005 K and a stability during measurement of 0.003 K. The measurements procedure in details is described elsewhere. Taking into account sources of error (calibration, measurements, impurities) the values of electrical and molar conductivity are thought to be certain within 0.05%.

The presented molar conductivities, Λ (Table S4), obtained from measured resistivity, r, ($\Lambda = 1/(rc)$) were calculated and analyzed in the frame work of the low-concentration chemical

model (lcCM) of Barthel, which describes thermodynamic and transport properties of aqueous solutions of 1:1 electrolytes up to 0.15 mol dm^{-3}. This approach uses the set of equations:

$$\frac{\Lambda}{\alpha} = \Lambda_o - S\sqrt{\alpha c} + E\alpha c \ln(\alpha c) + J_1 \alpha c - J_2 (\alpha c)^{3/2} \quad (1)$$

where

$$K_A^\circ = \frac{1-\alpha}{\alpha^2 c (y'_\pm)^2}; \; y'_\pm = \exp\left(-\frac{\kappa_D q}{1 + \kappa_D R}\right); \quad (2)$$

$$\kappa_D^2 = 16\pi N_A q \alpha c; \; q = \frac{e^2}{8\pi \varepsilon_0 \varepsilon k_B T} \quad (3)$$

where Λ_o is the molar conductivity at infinite dilution, $(1 - \alpha)$ is the fraction of oppositely charged ions bound in ion pairs, and K_A° is the standard-state (infinite dilution) association constant. The activity coefficients of the free cations, y'_+, and anions, y'_-, define, $(y'_\pm)^2 = y'_+ y'_-$; κ_D is the Debye parameter, e the proton charge, ε is the relative permittivity of the solvent, ε_o is the permittivity of vacuum, and T is temperature in Kelvin; k_B and N_A are the Boltzmann and Avogadro constants, respectively.

The lcCM model counts two oppositely charged ions as an ion pair if their mutual distance, r, is within the limits $a \leqslant r \leqslant R$, where a is the distance of closest approach of cation and anion, and R representing the distance up to which oppositely charged ions can approach as freely moving particles in the solution. Expressions of the coefficients S, E, J_1 and J_2 of Eq. (1) are given by Barthel et al. The limiting slope, S, and the parameter E are fully defined by the known data for the density, ρ_s, viscosity, η, and relative permittivity, ε, of the water. The coefficients J_1 and J_2 are functions of the distance parameter, R.

Important input parameters for the data analysis are the integration limits a and R. The lower limit, $a = a_+ + a_-$, of the association integral was calculated from the ionic radius of Cl$^-$, $a_- = 0.181$ nm, and of cations, $a_+ = 0.343$ nm, 0.339 nm, 0.340 nm, 0.337 nm and 0.361 nm for [OHC$_2$OC$_2$mim]$^+$, [OHC$_3$mim]$^+$, [OHC$_3$eim]$^+$, [OHC$_2$mim]$^+$, [C$_2$OC$_2$mim]$^+$, respectively. The chosen a_+ corresponds was obtained from DFT calculations, performed in this work.

3. Computational methods

All molecular dynamics (MD) simulations were performed using the Desmond 14.2 (Schrödinger Release and Desmond, 2015) and Jaguar 8.7 program, (Schrödinger Release and Jaguar, 2015) as implemented in Schrödinger Material Suite 2015-2 package with 256 pairs of cations and Cl$^-$ in a cubic box with periodic boundaries. A many body polarizable force field, developed by Borodin were used within NPT ensemble class. (Borodin, 2009) Several short simulations of about 100 ps were run in which partial charges were varied in order to equilibrate the system at target temperature (298.15 K) and pressure (1.01325 bar).
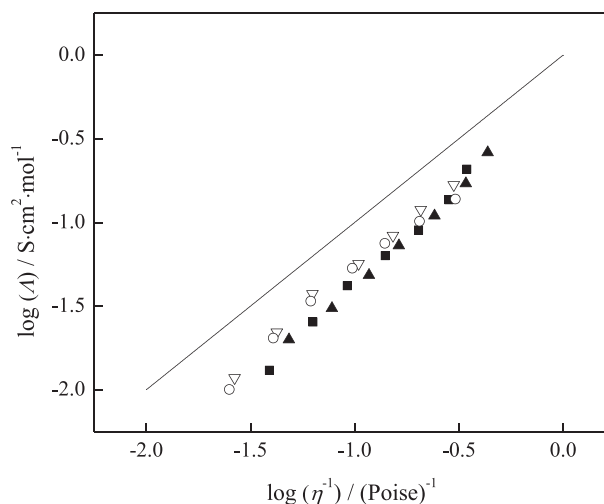
The total simulation time was 50 ns. Initially, IL was subjected to MD simulation with simulation time of 10 ns. During this first part, simulation model was relaxed in the beginning of simulation (meaning that for certain simulation time system was optimized within NVT ensemble). After that, using a checkpoint file, simulation was continued under the same con-

Table 1 Density, conductivity and viscosity of pure ionic liquids in temperature range 293.15–323.15 K at atmospheric pressure.

T/K	$\rho/\text{g cm}^{-3}$	$\kappa/\text{mS cm}^{-1}$	$\eta/\text{ mPa s}$
	[OHC$_2$OC$_2$mIm][Cl]		
293.15	1.22553	0.070	3761.98
298.15	1.22252	0.131	2363.35
303.15	1.21939	0.222	1593.71
308.15	1.21623	0.336	957.31
313.15	1.21305	0.495	655.23
318.15	1.20988	0.707	481.14
323.15	1.20664	0.994	334.51
	[C$_2$OC$_2$mIm][Cl]		
293.15	1.15326	0.121	2063.10
298.15	1.15024	0.185	1284.36
303.15	1.14711	0.292	852.26
308.15	1.14402	0.438	612.73
313.15	1.14186	0.659	413.43
318.15	1.13869	1.022	292.63
323.15	1.13597	1.563	229.83
	[OHC$_3$mIm][Cl]		
293.15	1.21638	0.064	3993.53
298.15	1.21334	0.130	2455.81
303.15	1.21019	0.215	1623.83
308.15	1.20784	0.338	1025.12
313.15	1.20481	0.474	715.63
318.15	1.20186	0.640	488.54
323.15	1.19894	0.869	328.26
	[OHC$_3$eIm][Cl]		
293.15	1.19421	0.082	2563.01
298.15	1.19109	0.159	1584.36
303.15	1.18802	0.261	1082.26
308.15	1.18499	0.394	712.73
313.15	1.18196	0.558	493.34
318.15	1.17801	0.844	352.21
323.15	1.17506	1.284	289.89

Standard uncertainties are: $u(\rho) = 7.2 \cdot 10^{-4} \text{ g cm}^{-3}$, $u(T) = 0.015 \text{ K}$. Relative standard uncertainties: $u_r(\eta) = 0.01$; $u_r(\kappa) = 0.01$; $u_r(p) = 0.015$.

Fig. 1 Walden plot in temperature range 293.15–323.15 K, (■), [OHC$_3$eIm][Cl]; (○),[OHC$_3$mIm][Cl]; (▲),[C$_2$OC$_2$mIm][Cl]; (▽), [OHC$_2$OC$_2$mIm][Cl].

Schrödinger Material Suite. Radial distribution function (RDF) analysis was performed with corresponding module of Material Suite, as well. The spatial distributions were analyzed from simulations trajectory, using TRAVIS software. (Brehm and Kirchner, 2011)

3.1. Structure functions

The total structure function $S(q)$ of the liquid was calculated using the equation:

$$S(q) = \frac{\rho_o \sum_i^n \sum_j^n x_i x_j f_i(q) f_j(q) \int_0^\infty 4\pi r^2 (g_{ij}(r) - 1) \frac{\sin qr}{qr} dr}{\left[\sum_i^n x_i f_i(q)\right]^2} \quad (4)$$

where $g_{ij}(r)$ is the radial pair distribution function for atmos of type i and j; x_i is the fraction of atom of type i; $f_i(q)$ is the X-ray atomic form factor for the ith type atom; and ρ_o is the number density. The Lorch window function is used to reduce the effect of finite truncation of $g(r)$ at large values of r.

The total structure factor $S(q)$ can be partitioned into ionic contribution:

$$S(q) = S_{c-c}(q) + S_{a-c}(q) + S_{c-a}(q) + S_{a-a}(q) \quad (5)$$

where a and c are anionic and cationic contribution, respectively.

ditions for additional 40 ns, during which data necessary for calculation of bulk properties was sampled. DFT calculations of examined systems were performed employing B3LYP exchange – correlation functional (B3LYP-D3) and 6-31 + G (d,p) basis set. System of ion pairs was prepared employing Disordered System Builder module, while bulk properties were analyzed with MS MD Trajectory Analysis module of

Table 2 Values of activation energy (E) and glass transition temperature (T_o) obtained using VFT equation.

ILs	Viscosity		Conductivity	
	$E/\text{kJ mol}^{-1}$	T_o/K	$E/\text{kJ·mol}^{-1}$	T_o/K
[OHC$_2$OC$_2$mIm][Cl]	923.63	202.82	922.17	205.21
[C$_2$OC$_2$mIm][Cl]	837.05	216.74	813.82	218.91
[OHC$_3$mIm][Cl]	940.42	203.03	925.17	205.11
[OHC$_3$eIm][Cl]	842.92	211.64	863.33	216.75

Table 3 Experimental and simulated densities for pure ionic liquids at temperature 298.15 K and calculated ion pair binding energies (*IPBE*) between cation and anion.

ILs	ρ (exp.)/g cm^{-3}	ρ (sim.)/g·cm^{-3}	RSD[a]/%	$IPBE$/kJ mol^{-1}
[OHC$_2$OC$_2$mIm][Cl]	1.22524	1.22458	0.5	−420.49
[C$_2$OC$_2$mIm][Cl]	1.15024	1.14997	0.3	−391.62
[OHC$_3$mIm][Cl]	1.21334	1.21283	0.4	−416.31
[OHC$_3$eIm][Cl]	1.19109	1.19072	0.3	−409.28

[a] $RSD = 100((\rho(\exp) - \rho(\sim))/\rho(\exp))$.
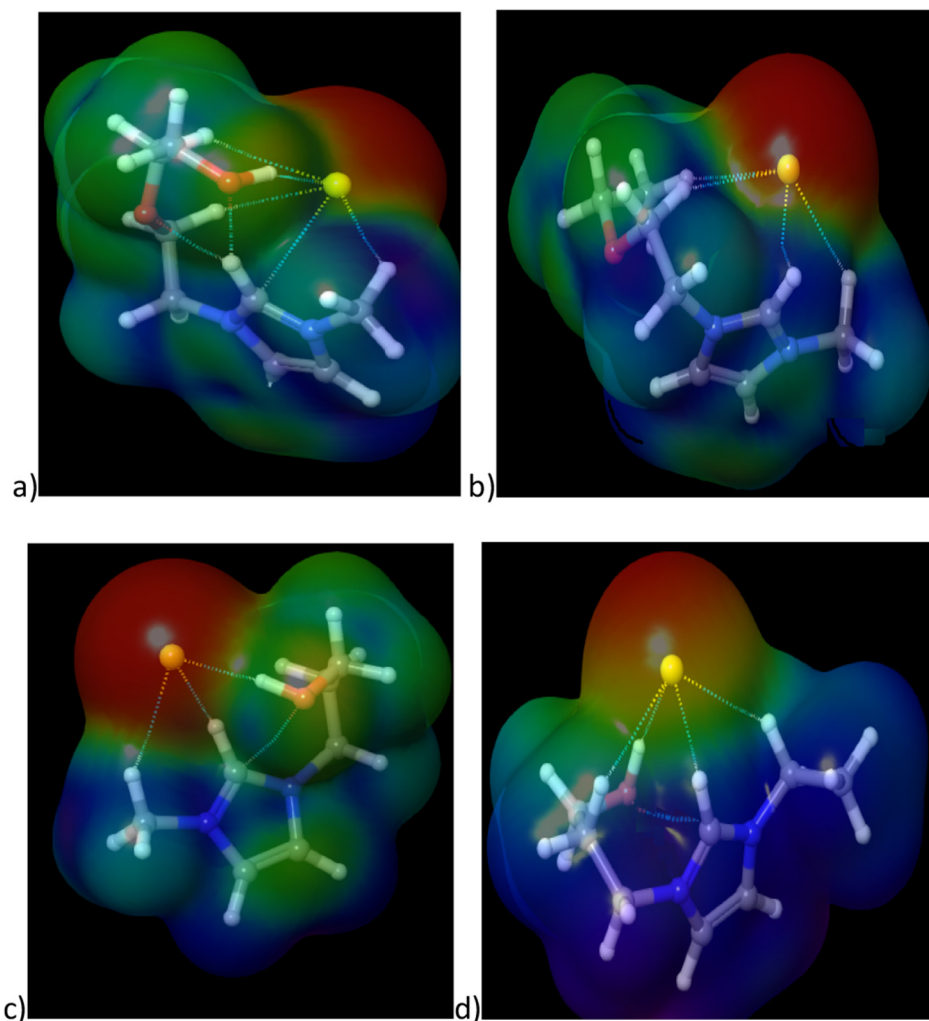
Fig. 2 MEP surfaces for investigated ionic liquids: (a) [OHC$_2$OC$_2$mIm][Cl], (b) [C$_2$OC$_2$mIm][Cl], (c) [OHC$_3$mIm][Cl], (d) [OHC$_3$eIm][Cl].

4. Results and discussion

4.1. Pure ionic liquids

Density, viscosity and conductivity of pure chloride based ionic liquids, were measured at temperature range from 293.15 K to 323.15 K. The results are tabulated in Table 1.

Variation of viscosity and conductivity with temperature (Figs. S9 and S10) are fitted using Vogel–Fulcher–Tammann (VFT) equation (Fulcher, 1925):

$$A = A_o \exp(E/(T - T_o)) \tag{6}$$

where A is the viscosity or conductivity, T is the temperature in K, and A_o is coefficient of VFT equation, E is activation energy and T_o is glass transition temperature. Obtained values for activation energies and glass transition temperature are presented in Table 2.

From Table 2 it can be seen that higher activation energies are obtained for [OHC$_2$OC$_2$mIm][Cl] and [OHC$_3$mIm][Cl], comparing to [OHC$_3$eIm][Cl] and [C$_2$OC$_2$mIm][Cl].

Based on experimental values of viscosity and conductivity, Walden plot was applied, in order to examine ionicity of synthesized ionic liquids. The relation between molar conductivity and viscosity can be demonstrated by equation:

$$\log \Lambda_m = \log C + \alpha \log \eta^{-1} \tag{7}$$

where Λ_m is molar conductivity, η^{-1} is fluidity, α is slope of the line in the Walden plot which reflects the decoupling of the ions, C "is Walden product of fractional Walden rule". The Walden plot is presented on Fig. 1 and shows thet all synthesized ionic liquids are below ideal KCl line.

In order to quantify ionicity, Angell method (MacFarlane et al., 2009) was applied by measuring the vertical distance from ionic liquids line to the KCl line. Obtained results at 298.15 K for ionicity of all examined ILs ranged between 40 and 60%, indicating stronger interactions between cation and anion, causing higher level of association for this ionic liquid. (MacFarlane et al., 2009)

With a goal to prove experimental results and to better understand why this chloride ionic liquids are liquid at room temperature computational simulations are performed. First step was checking validity of force fields by comparing experimental density with densities obtained from MD simulations. The results are presented in Table 3.

The agreement between computation and experimental determined densities is quite good with a maximum deviation less than 1%.

Ion pair binding energy (IPBE) is important quantity and can be correlated with physico-chemical properties of ILs such as melting point, thermal stability and transport properties

(Roohi and Khyrkhah, 2013). The values of calculated IPBE for investigated ionic liquids are given in Table 3. As can be seen from Table 3 values of IPBE follow the order [OHC$_2$OC$_2$mIm][Cl] < [OHC$_3$mIm][Cl] < [OHC$_3$eIm][Cl] < [C$_2$OC$_2$mIm][Cl]. Comparing experimental results for pure ionic liquids and IPBE it is noted that ionic liquids with lowest value of IPBE have a highest values of viscosity and density and lowest conductivity. This is in accordance with correlations made by Bernard et al. (2010) Namely, ion pair binding energy indicate the strength of the intermolecular interaction between ions. Lower value of IPBE points to stronger molecular packaging, suggesting higher value of density and viscosity, as in the case of investigated ionic liquids (Bernard et al., 2010)

In an ionic liquid system, cation-anion interactions are largely determined by the balance among electrostatic properties, van der Waals interactions, and the geometrical properties of both cations and anions. Fig. 2 shows the molecular electrostatic potentials (MEP) for all ionic liquids. The negative (red) regions of the molecular electrostatic potential are related to the electrophilic reactivity and the positive (blue) regions are related to the nucleophilic reactivity.

It is evident that positive electrostatic potential is mostly located around imidazolium ring, with highest values for hydrogen atoms on the imidazolium ring as well as methyl group. Due to the high potential this part of cation are favorable for interactions with anions. The imidazolium hydrogens, should additionally be able to form hydrogen bonds. In particular, a positive electrostatic potential was found around the carbons on the imidazolium ring, especially at C2. This makes them different from traditional hydrogen donors, such as
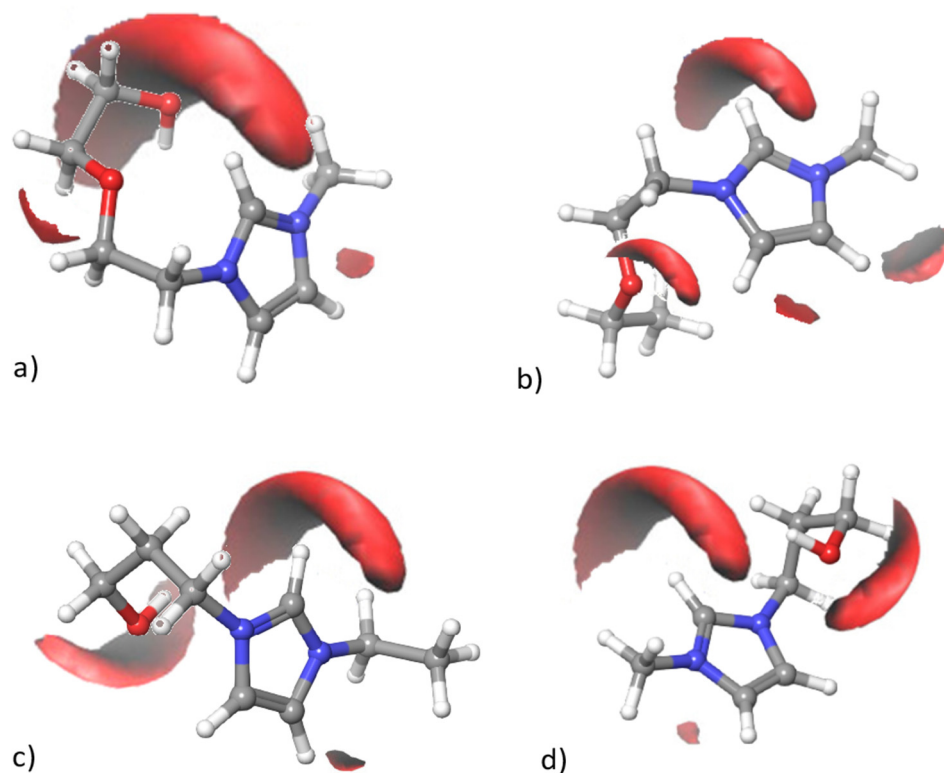

Fig. 3 Spatial distribution function for probability of chloride anion (red surfaces) around cations: (a) [OHC$_2$OC$_2$mIm][Cl]; (b) [C$_2$OC$_2$mIm][Cl]; (c) [OHC$_3$eIm][Cl]; (d) [OHC$_3$mIm][Cl].
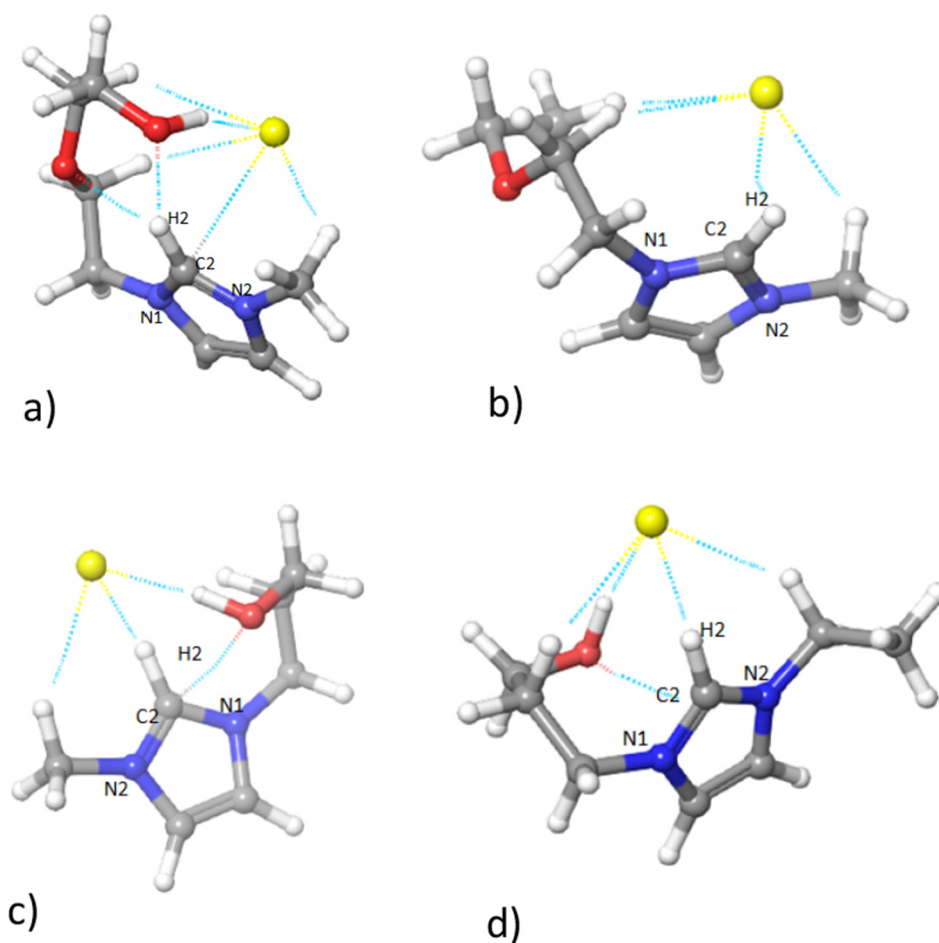
Fig. 4 Optimized structure of monomers, with represent non-covalent interactions and numeration of most significant atoms for discussion: (a) [OHC$_2$OC$_2$mIm][Cl], (b) [C$_2$OC$_2$mIm][Cl], (c) [OHC$_3$mIm][Cl], (d) [OHC$_3$eIm][Cl].

Table 4 Bond length between chloride anion and hydrogen H2 from different IL cation, charge density (ρ) around H2 for investigated ionic liquids.

ILs	$r_{\text{Cl–H2}}$ (Å)	ρ(H2)/e
[OHC$_2$OC$_2$mIm][Cl]	2.25	0.181
[C$_2$OC$_2$mIm][Cl]	1.98	0.226
[OHC$_3$mIm][Cl]	2.13	0.186
[OHC$_3$eIm][Cl]	2.02	0.166
[bmim][Cl]	1.84[45]	0.238[a]

[a] Obtained by same level of theory as oxygen based ionic liquids in this work.

oxygen from water, which typically bear a negative potential (Dinur, 1990; Wheatley and Harvey, 2007).

To additionally determine preference sites for interactions between anion and cation, spatial distribution function (SDF) was calculated. The results are presented in Fig. 3.

According to the probability density to find chloride anions around cations, two main types of cation-anion contact can be classified. The most prominent regions to find an anion is around H2 from imidazolium ring and oxygen atoms in alkyl side chain.

In order to get more detailed insight and to visualize interaction that occurs in investigated ILs, optimized structures of monomers are shown on Fig. 4, and a length of the bond between chloride anion and hydrogen atom H2 is presented in Table 4, along with ion pair binding energies and charge density around atom H2 from imidazolium ring.

As can be seen from Fig. 4 and Table 4, chloride anion, from who is expected to have strongest interactions with H2 hydrogen from imidazolium ring, is on longer distance that is usual in case of non-functionalized chloride ILs, for example [bmim][Cl]. (Zhang et al., 2012) These observations suggest that ionic liquids with oxygen in side chain form additional interactions between hydrogen from H2 and oxygen from side chain. This interaction creates competitions to chloride anion, causing self-chelating effect in investigated ionic liquids. As can be seen from Table 4 charge density around H2 decrease, due to interactions between oxygen from side chain and H2, causing weaker interactions between H2 and chloride.

Furthermore, more negative values of *IPBE* (Table 3), that describes overall energy of attraction between ions, indicate that ionic liquids with hydroxyl group have stronger interactions between cation and anion comparing to [C$_2$OC$_2$mIm][Cl]. The reason for this is additional interactions between hydrogen from OH group and chloride anion, contributing to higher binding energies.
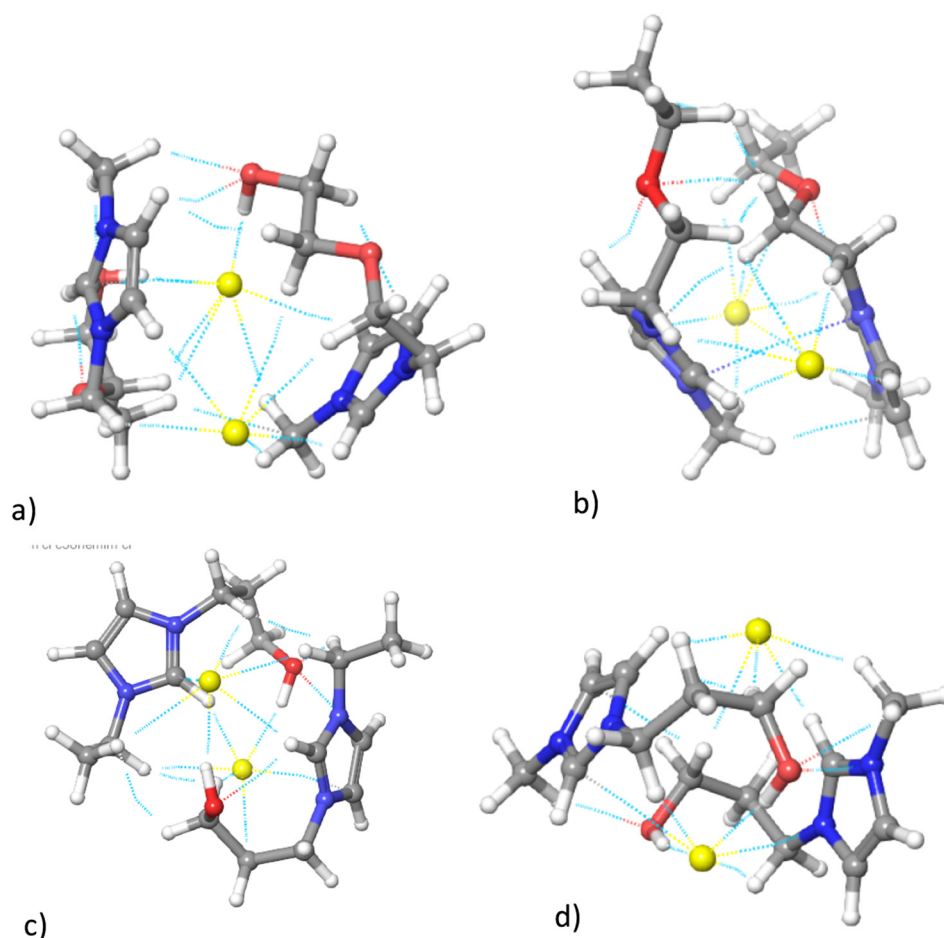
Fig. 5 Optimized structure of dimmers, with represent non-covalent interactions: (a) [OHC$_2$OC$_2$mIm][Cl], (b) [C$_2$OC$_2$mIm][Cl], (c) [OHC$_3$mIm][Cl], (d) [OHC$_3$eIm][Cl].
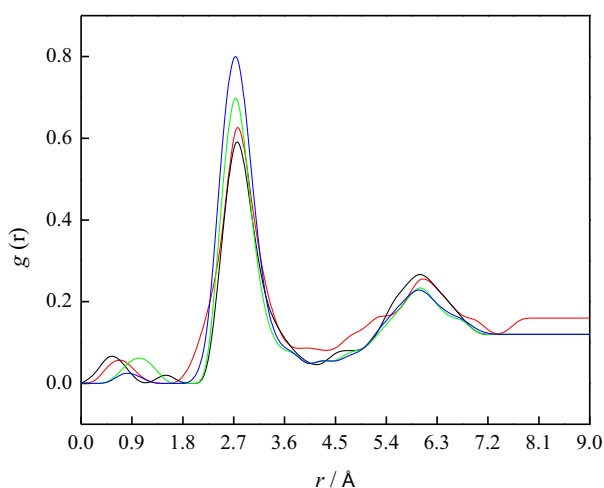
Fig. 6 RDFs of Cl$^-$ and H2 for pure ionic liquids on 298.15 K (green line [OHC$_2$OC$_2$mIm][Cl], blue line [C$_2$OC$_2$mIm][Cl], black line [OHC$_3$eIm][Cl], red line [OHC$_3$mIm][Cl],).

In order to even better understand organization and interactions that occur in investigated ILs, optimized dimmers are

represented in Fig. 5. From Fig. 5 is clearly evident that in ionic liquids functionalized with hydroxyl group, OH group interact both with H2 and with chloride, causing stronger attractive forces between cation and anion. On the other hand, because of these interactions center of charges are closer to each other inducing liquid state of ionic liquids.

To obtain information about distance between cations and anions, radial distribution function (RDFs) were calculated from molecular dynamics simulations. RDFs for anion and most acidic proton (H2) in all ionic liquids are presented in Fig. 6. From Fig. 6 it can be seen that highest values of $g(r)$ has ionic liquid [C$_2$OC$_2$mIm][Cl], and also maximum of $g(r)$ shows at lowest value of r. This behaviour indicate that chloride is closest to hydrogen H2 in case of [C$_2$OC$_2$mIm][Cl], since ether group from alkyl side chain had not significant influence on interaction between side chain of cation and anion. In the case of ionic liquids with OH group, position of $g(r)$ maximum value is changing. It can be noted that chloride is on longest distance to hydrogen H2 in [OHC$_3$eIm][Cl], indicating that additional ethyl group on imidazolium cation making H2 less exposed to anion due to steric hindrance.

Based on RDF results, structure functions were obtained, in order to separate anionic and cationic contribution and results are presented in Fig. 7. As can be seen from Fig. 7, almost the same contribution of cation-cation and cation-

anion to interaction in pure ionic liquid were noted in ionic liquids [OHC$_3$mIm][Cl], [OHC$_3$eIm][Cl], [OHC$_2$OC$_2$mIm][Cl]). Only in case of [C$_2$OC$_2$mIm][Cl] interactions between cation and anion are more pronounced comparing to cation-cation interactions, which are in consistence with our previous statements.

Adopting a color scheme (Fig. 8) to distinguish atoms belonging to the "charged" parts provides an excellent visual aid to perceive structural changes. (Canongia Lopes et al., 2004) As can be seen chlorides (represented in red colour) are concentrated in several groups of layers. Particularly, additional interaction between OH-groups and imidazolium H2 cause formation of separated cation and anion layers, which is responsible for liquid state of these ionic liquids.

4.2. Aqueous solutions

In order to discuss nature of interactions and structuring of water in the investigated ILs + water system, several important parameters may be obtained from the experimental density, viscosity and electrical conductivity. Using the values of V_ϕ from Table S2, the apparent molar volume at infinite dilution, $V_\Phi°$, can be derived applying Masson's equation (Masson, 1929):

$$V_\phi = V_\phi° + S_V \cdot \sqrt{c} \tag{8}$$

The variation of V_ϕ with concentration is presented on Fig. 9. The apparent molar volume at infinite dilution is an aditive value which includes partial contributions of cation and anion of the ionic liquid. Since the literature value of $V_\phi°$ for Cl$^-$ is 23.3 cm^3 mol^{-1} at 298.15 K (Marcus, 1993) the values of the apparent molar volume at infinite dilution are obtained for investigated cations and presented in Table 5. Here S_V is the Masson's coefficient tabulated in Table S5 along with $V_\phi°$. The negative values of S_V indicates weak ion-ion interactions in investigated systems. These interactions are weaker at higher temperatures.

From temperature dependence of apparent molar volume at infinite dilutions (Eq. (9)), values of limiting molar expansibility, $E_\phi°$ was calculated and results are presented in Table S6.

$$E_\phi° = \left(\frac{\partial V_\phi°}{\partial T}\right)_p = a_1 + 2a_2 T \tag{9}$$

Positive values of $E_\phi°$, which are increasing at higher temperature indicates that aqueous solutions of investigated ionic liquids expand greater than pure water.

Based on this results, Hepler's equation was used: (Hepler, 1969)

$$\left(\frac{\partial E_\phi°}{\partial T}\right)_p = \left(\frac{\partial^2 V_\phi°}{\partial T^2}\right)_p = 2a_2 \tag{10}$$

The Hepler's coefficient, obtained from second derivative of apparent molar volume at infinite dilution with temperature, was calculated and presented in Table 5. Obtained positive values for all investigated ILs indicates structure making properties.
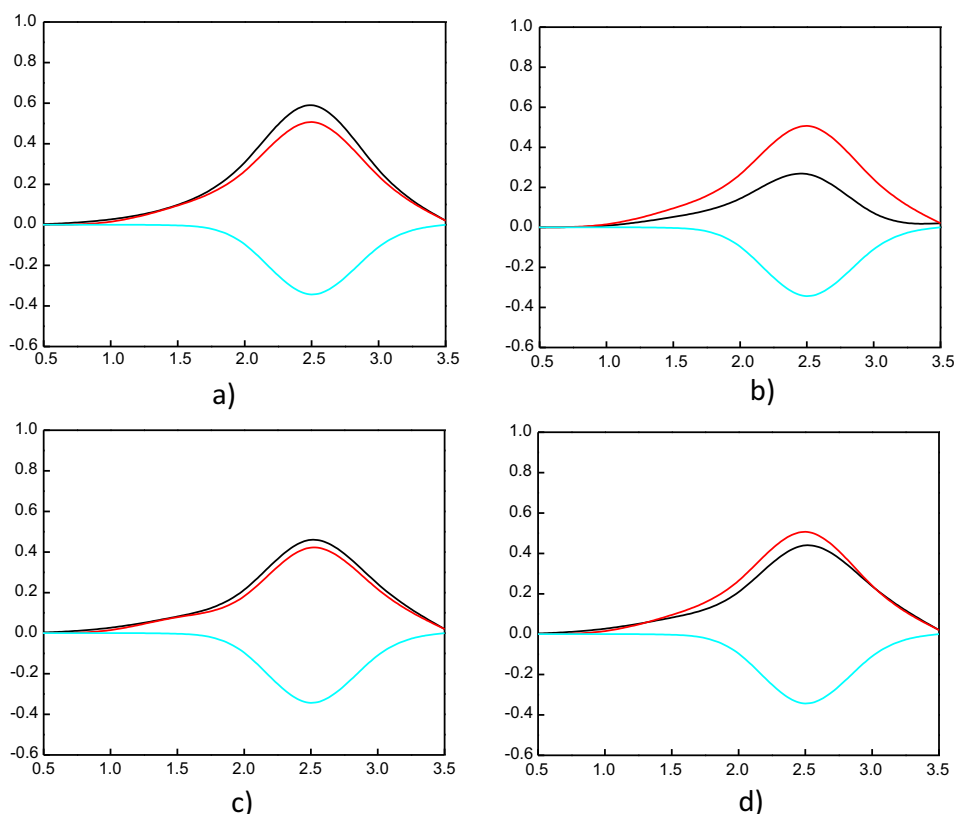

Fig. 7 Partioning of $S(q)$ to cation-cation (black line), cation-anion (red line) and anion-anion (blue line) correlations: (a) [OHC$_2$OC$_2$mIm][Cl], (b) [C$_2$OC$_2$mIm][Cl], (c) [OHC$_3$mIm][Cl], (d) [OHC$_3$eIm][Cl].
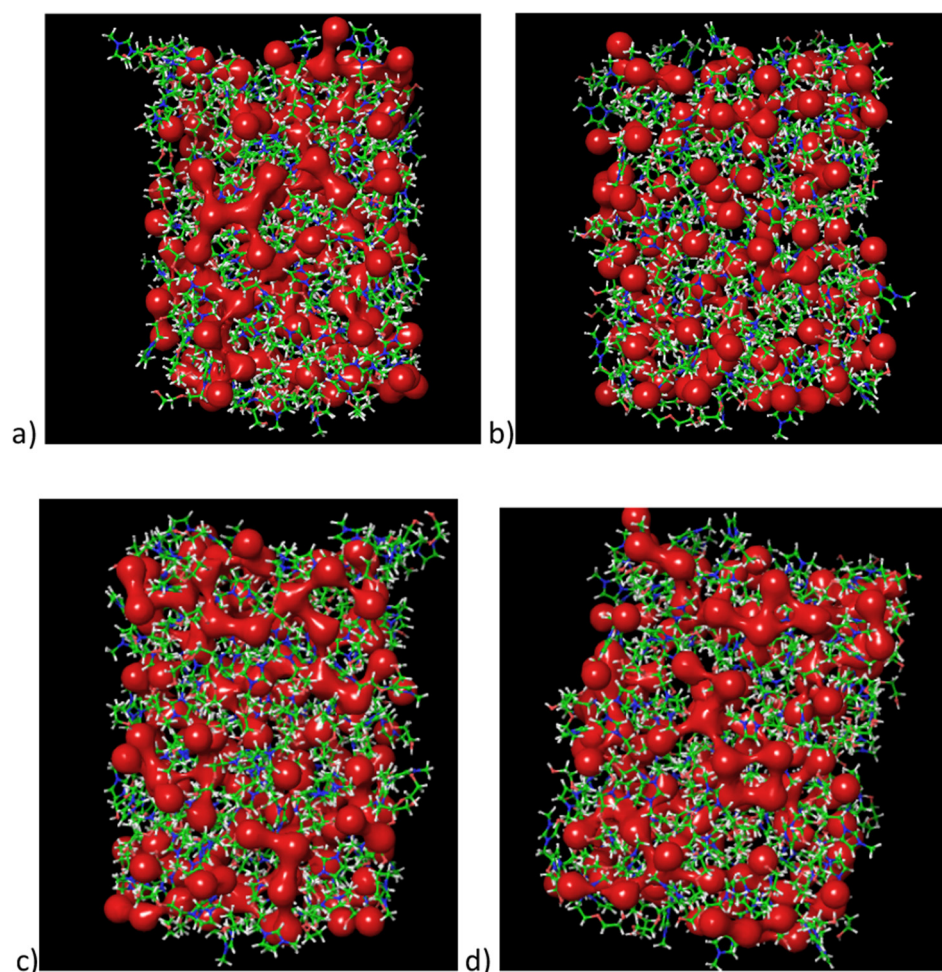
Fig. 8 Color sheme for distinguish organization of chloride (red colour): (a) [OHC$_3$mIm][Cl], (b) [OHC$_3$eIm][Cl], (c) [OHC$_2$OC$_2$mIm][Cl]), (d) [C$_2$OC$_2$mIm][Cl].
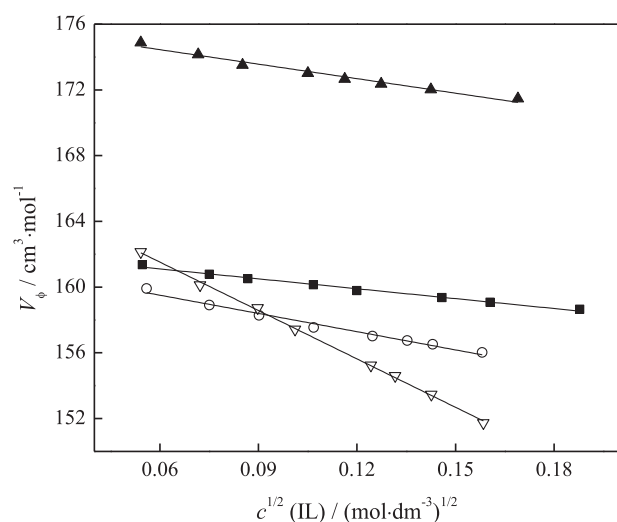

Fig. 9 Variation of apparent molar volume with concentration, (∇), [OHC$_2$OC$_2$mIm][Cl]; ($\blacktriangle$),[C$_2$OC$_2$mIm][Cl]; ($\blacksquare$), [OHC$_3$eIm][Cl]; ($\circ$),[OHC$_3$mIm][Cl].

Table 5 Values of apparent molar volume at infinite dilution, V_ϕ°, for cations at 298,15 K, and Hepler's coefficient.

	V_ϕ° (cation)/cm^3 mol^{-1}	Hepler's coefficient/cm^3 mol^{-1} K^{-1}
[OHC$_2$OC$_2$mIm]$^+$	144.10	0.0056
[C$_2$OC$_2$mIm]$^+$	152.83	0.0036
[OHC$_3$mIm]$^+$	139.39	0.0039
[OHC$_3$eIm]$^+$	139.01	0.0041

The experimental results of the viscosity for aqueous solutions were fitted in function of IL concentration using the Jones–Dole equation: (Jones and Dole, 1929)

$$\frac{\eta}{\eta_{\mathrm{o}}} = 1 + A\sqrt{c} + Bc \qquad (11)$$

where η_{o} is the viscosity of pure water, $A\sqrt{c}$ term (coefficient A is presented in Table S7) is identical to those obtained from a limiting–law theory of long–range electrostatic interactions in a dielectric continuum. The viscosity coefficient B was found

Table 6 Values of viscosity B-coefficient at different temperatures.

T/K	$[OHC_2OC_2mIm][Cl]$	$[C_2OC_2mIm][Cl]$	$[OHC_3mIm][Cl]$	$[OHC_3eIm][Cl]$
	$B/dm^3 \cdot mol^{-1}$			
278.15	0.555	0.572	0.511	0.476
283.15	0.548	0.568	0.509	0.474
288.15	0.541	0.559	0.505	0.469
293.15	0.533	0.550	0.499	0.463
298.15	0.525	0.543	0.493	0.456
303.15	0.513	0.537	0.486	0.449
308.15	0.500	0.531	0.479	0.440
313.15	0.482	0.502	0.470	0.429

Table 7 Hydration number of oxygen functionalized ionic liquids.

ILs	h_n
$[OHC_2OC_2mIm][Cl]$	5.62
$[C_2OC_2mIm][Cl]$	6.61
$[OHC_3mIm][Cl]$	3.60
$[OHC_3eIm][Cl]$	3.41
$[OHC_2mim][Cl]$[33]	1.96

to be an additive property of ions and gives a useful measure of ion–solvent interactions. Variations of B-coefficient with temperature are presented in Table 6.

Positive values of the coefficient B indicate strong interactions between ions and water molecules, or structure-making effect. Additional criteria to describe structure-making or structure-breaking tendency in the system is variation of the coefficient B with temperature, namely dB/dT. Negative value of dB/dT for all investigated ionic liquids is a characteristic of structure-making ions. From the calculated B values in this work and literature value for $[Cl]^-$, $-0.005\ dm^3\ mol^{-1}$ at the same temperature, (Masson, 1929), the contribution of $[OHC_2OC_2mIm]^+$, $[C_2OC_2mIm]^+$, $[OHC_3mIm]^+$ and $[OHC_3eIm]^+$ are 0.548, 0.530, 0.498 and 0.461 $dm^3\ mol^{-1}$ respectively. Comparing obtained results with B coefficient for $[bmim]^+$ of 0.453 $dm^3\ mol^{-1}$ at 298.15 K, (Marcus, 2009) higher values of B coefficients indicate better structure making properties of investigated cations. However, values of viscosity coefficient B are not significantly higher comparing to $[bmim]^+$ as was expected due to presence of OH groups in side chain, which can form hydrogen bond with water. Furthermore, it was found that B-coefficient for 1-(2-hydroxyethyl)-3-methylimida

zolium chloride (0.228 $dm^3\ mol^{-1}$ at 298.15 K) is smaller than in case of $[bmim]^+$. (Vraneš et al., 2016) These observations imply that formation of H-bonds between OH groups from side chain and chloride anion significantly reduce ability of molecule to interact with water. In order to examine validity of experimental results and to better understand interactions with water, molecular dynamics simulations were performed for aqueous solution of IL. Number of ions was set to match experimental concentration 0.04 mol dm^{-3}. From MD simulations, radial distribution function was calculated and results for interactions between H2 atoms from ILs and water center of mass are presented in Fig. 10.

As can be seen from Fig. 10, water is closest to $[C_2OC_2mIm][Cl]$, indicating strongest interactions and highest availability of H2 atom from imidazolium cation in case of this ionic liquid. This observation suggests that chloride ionic liquid functionalized only with ether group in alkyl chain have weakest tendency to form additional interaction between side chain and imidazolium ring. On the other hand, for all three ionic liquids with hydroxyl group in alkyl chain, maximum value of RDF is at significantly lower distance, suggesting weaker interaction between water and acidic proton from imidazolium ring. This is in agreement with our previous statement that side chain of cation cause self-chelating effect, via formation of additional interaction between hydroxyl group and H2.

In order to quantify interactions between ionic liquids and water, hydration number was calculated for all investigated ionic liquids, as well as previously published 1-(2-hydroxyethyl)-3-methylimidazolium chloride. Hydration number, h_n of water molecules associated with one molecule of solute have been estimated by using the equation:

Table 8 Values of association constants at different temperatures.

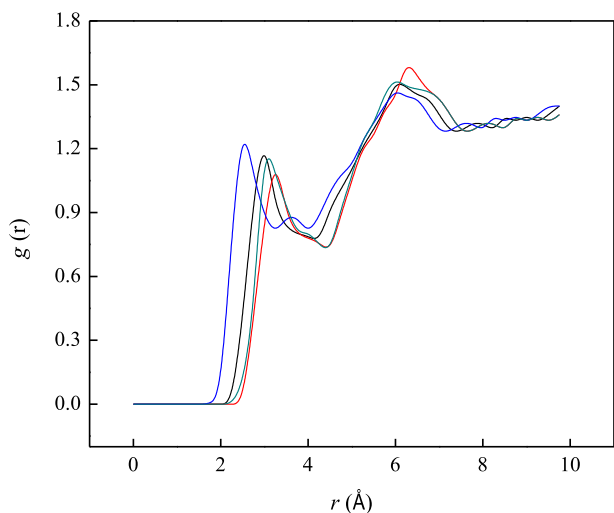| T/K	$[OHC_2OC_2mIm][Cl]$	$[C_2OC_2mIm][Cl]$	$[OHC_3mIm][Cl]$	$[OHC_3eIm][Cl]$
	$K_A^\circ/dm^3\ mol^{-1}$			
278.15	8.23	7.83	8.06	8.21
283.15	8.22	7.82	8.11	8.26
288.15	8.19	7.82	8.18	8.30
293.15	8.17	7.81	8.19	8.33
298.15	8.12	7.81	8.20	8.37
303.15	8.10	7.80	8.23	8.43
308.15	8.09	7.79	8.26	8.57
313.15	8.06	7.78	8.35	8.63

Fig. 10 RDFs for H2 of ILs with water molecules center of mass (green line [OHC$_2$OC$_2$mIm][Cl], blue line [C$_2$OC$_2$mIm][Cl], black line [OHC$_3$eIm][Cl], red line [OHC$_3$mIm][Cl]).
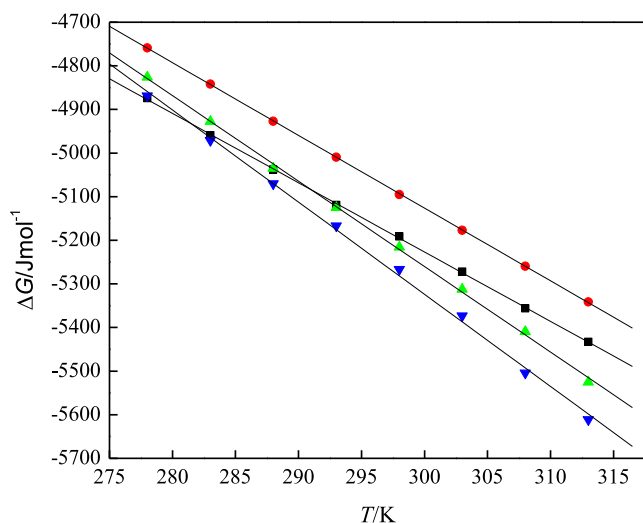

Fig. 11 Gibbs free energy (ΔG_A^o) of ion pair formation as a function of temperature, $T = (278.15–313.15)$ K for systems: (green [OHC$_2$OC$_2$mIm][Cl], blue [C$_2$OC$_2$mIm][Cl], black [OHC$_3$-eIm][Cl], red [OHC$_3$mIm][Cl]).

$$h_n = \frac{V_e^o - V_\phi^o}{V_m(H_2O)} \quad (12)$$

where V_e^o is the limiting value of the effective volume of the flowing unit (solute + H$_2$O), calculated from Thomas equation, (Thomas, 1965) $V_m(H_2O)$ is the molar volume of water and values of apparent molar volume is given in Table S2. Obtained results for hydration number are presented in Table 7.

As can be seen from Table 7, ionic liquid [C$_2$OC$_2$mIm][Cl] have a highest hydration number. On the other hand, ionic liquids substituted only with hydroxyl group in side chain have a significantly lower h_n. Based on hydration numbers, volumetric and viscosimetric measurements, and results of molecular simulations it is obvious that OH group in side chain will not promote structure making properties. Due to interactions

Table 9 The values of enthalpy (ΔH_A^o) and entropy (ΔS_A^o) for investigated ILs obtained from ΔG_A^o.

IL	ΔS_A^o J·K^{-1}mol^{-1}	ΔH_A^o J·mol^{-1}
[OHC$_2$OC$_2$mIm][Cl]	15.89	−460.35
[C$_2$OC$_2$mIm][Cl]	16.66	−127.06
[OHC$_3$mIm][Cl]	19.59	616.84
[OHC$_3$eIm][Cl]	21.13	1014.15

between OH group and H2 from imidazolium ring, interactions with water will become weaker. On the other hand, in ionic liquids with only ether group in side chain, H2 from imidazolium ring will be available for interaction with water. This will promote structure making tendency of this ionic liquids, along with hydrophobic solvation of alkyl chain. It is evident from this results, that functionalization with hydroxyl group not contribute to structure making properties of ionic liquids, which can be extremely important for formation of ABS systems, where structure making ability is main contribution for formations of these systems. (Ventura et al., 2011)

Because of lack of literature data for association constants (K_A) of tis ionic liquids, conductivity measurements of aqueous solutions were conducted. Since $\Lambda_o = \lambda_o^+ + \lambda_o^-$, limiting conductivities for cations can be calculated from the observed Λ_o results using appropriate literature values of λ_o^-. The values obtained for λ_o^+ are summarized in Table S8.

Based on experimental results of molar conductivity and applying lcCM model, association constant for examined ionic liquids was calculated. Obtained values for association constants (K_A^o) and their variation with temperature are presented in Table 8.

How can be seen from Table 8, there is two different trends in the investigated ILs. The association constants are the lowest for aqueous solutions of [C$_2$OC$_2$mIm][Cl] and they are decreasing with the temperature. Similar trend is noted in another system with ether functional group, [OHC$_2$OC$_2$mIm][Cl]. In other hand, for ionic liquids substituted only with –OH group, association constant increase with temperature. Comparing this results with association constants for [bmim][Cl] obtained in work of Shekaari and Mousavi., (Shekaari and Mousavi, 2009) values at 298.15 and 308.15 K are similar ($K_A^o = 7.92$ and 8.37 respectively).

From the temperature dependence of the K_A^o, Gibbs free energy (ΔG_A) of ion pair formation was calculated:

$$\Delta G_A^o(T) = \Delta H_A^o - T\Delta S_A^o = -RT \ln K_A(T) \quad (13)$$

The corresponding entropy, $\Delta S_A^o = -(\partial \Delta G_A^o/\partial T)_p$ and enthalpy, $\Delta H_A^o(T) = \Delta G_A^o + T\Delta S_A^o$, of ion association at atmospheric pressure was obtained from changes of free Gibbs energy with temperature.

The values of ΔG_A^o presented in Fig. 11 and corresponding entropy and enthalpy are tabulated in Table 9. The ΔG_A^o are negative for all examined ionic liquid and indicates that the formation of ion pairs is a spontaneous process.

From Table 9 it can be seen thet all investigated ILs have positive values of ΔS_A^o. This indicating that transition from the free solvated ions into the ion pair causes that system becomes less ordered. The negative values of ΔH_A^o for ionic liquid with ether group indicate that the ion pair forming pro-

cesses is exothermic. On the other hand, ionic liquids substituted only with OH group have positive values of ΔH_A^o, indicating endothermic process of ion pair formation.

5. Conclusions

In this paper four oxygen functionalized imidazolium based ionic liquids with chloride anion, which are liquid at room temperature, were synthesized. Applying both experimental and computational approach, pure ionic liquids were investigated. Computational analysis based on both DFT calculations and MD simulations gave an additional insight into the interactions between constituting ions understanding better the interactions in ILs, responsible for liquid state. Additionally, diluted aqueous solutions of ionic liquids were also examined by measuring viscosity, density and electrical conductivity. Based on these results, along with molecular simulations, structuring of water in presence of investigated ILs is discussed. It was noted that existence of hydroxyl group not promoted structure making properties in way as it expected, due to interactions between OH group and H2 from imidazolium cation. From electrical conductivity measurements, constant of association were obtained applying low concentration conductivity model. Concluding all results, interactions between functionalized side chain and imidazolium ring of cation was determined to be main reason for liquid state.

Acknowledgements

Appendix A. Supplementary material

Supplementary data associated with this article can be found, in the online version, at https://doi.org/10.1016/j.arabjc.2017.12.011.

References

Barthel, J., Feuerlein, F., Neueder, R., Wachter, R., 1980. Calibration of conductance cells at various temperatures. J. Solution Chem. 9, 209–219.

Bernard, U.L., Izgorodina, E.I., MacFarlane, D.R., 2010. New insights into the relationship between ion-pair binding energy and thermodynamic and transport properties of ionic liquids. J. Phys. Chem. C 114, 20472–20478.

Bešter-Rogač, M., Stopa, A., Hunger, J., Hefter, G., Buchner, R., 2011. Association of ionic liquids in solution: a combined dielectric and conductivity study of [bmim][Cl] in water and in acetonitrile. Phys. Chem. Chem. Phys. 13, 17588–17598.

Branco, L.C., Rosa, J.N., Moura Ramos, J.J., Afonso, C.A.M., 2002. Preparation and characterization of new room temperature ionic liquids. Chem. Eur. J. 8, 3671–3677.

Brehm, M., Kirchner, B., 2011. TRAVIS – a free analyzer and visualizer for Monte Carlo and Molecular Dynamics trajectories. J. Chem. Inf. Model. 51, 2007–2023.

Borodin, O., 2009. Polarizable force field development and molecular dynamics simulations of ionic liquids. J. Phys. Chem. B 113, 11463–11478.

Canongia Lopes, J.N., Deschamps, J., Pádua, A.A.H., 2004. Modeling ionic liquids using a systematic all-atom force field. J. Phys. Chem. B 108, 2038–2047.

Choi, S., Kim, K.S., Yeon, S.H., Cha, J.H., Lee, H., Kim, C.J., Yoo, I. D., 2007. Fabrication of silver nanoparticles via self-regulated reduction by 1-(2-hydroxyethyl)-3-methylimidazolium tetrafluoroborate. Korean J. Chem. Eng. 24, 856–859.

Coadou, E., Goodrich, Neale, A.R., Timperman, L., Hardacre, C., Jacquemin, J., Anouti, M., 2016. Synthesis and Thermophysical properties of ether functionalized sulfonium ionic liquids as potential electrolytes for electrochemical applications. ChemPhysChem 17, 3992–4002.

Deng, Y., Besse-Hoggan, P., Sancelme, M., Delort, A.M., Husson, P., Costa Gomes, M.F., 2011. Influence of oxygen functionalities on the environmental impact of imidazolium based ionic liquids. J. Hazard. Mater. 198, 165–174.

Dinur, U., 1990. "Flexible" water molecules in external electrostatic potentials. J. Phys. Chem. 94, 5669–5671.

Domanska, U., Marciniak, A., 2005. Liquid phase behaviour of 1-hexyloxymethyl-3-methyl-imidazolium-based ionic liquids with hydrocarbons: the influence of anion. J. Chem. Thermodyn. 37, 577–585.

Dreyer, S., Kragl, U., 2008. Ionic liquids for aqueous two-phase extraction and stabilization of enzymes. Biotechnol. Bioeng. 99, 1416–1424.

Fan, Y., Li, X., Zhang, L., Duan, P., Li, F., Zhao, D., Wang, Y., Wu, H., 2017. Ether-functionalized ionic liquids: Highly efficient extractants for hordenine. Chem. Eng. Res. Design 124, 66–73.

Fang, S., Yang, L., Wang, J., Li, M., Tachibana, K., Kamijima, K., 2009. 2009, Ionic liquids based on functionalized guanidinium cations and TFSI anion as potential electrolytes. Electrochim. Acta 54, 4269.

Fareghi-Alamdari, R., Nadiri Niri, M., Hazarkhani, H., 2017. Synthesis and characterization of a new hydroxyl functionalized diacidic ionic liquid as catalyst for the preparation of diester plasticizers. J. Mol. Liq. 227, 153–160.

Fei, Z., Geldbach, T.J., Zhao, D., Dyson, P.J., 2006. From dysfunction to bis-function: on the design and applications of functionalised ionic liquids. Chem. Eur. J. 12, 2122–2130.

Fulcher, G.S., 1925. Analysis of recent measurements of the viscosity of glasses. J. Am. Ceram. Soc. 8, 339–355.

Hallett, J.P., Welton, T., 2011. Room-temperature ionic liquids: solvents for synthesis and catalysis. 2. Chem. Rev. 111, 3508–3576.

Han, H.B., Nie, J., Liu, K., Li, W.K., Feng, W.F., Armand, M., Matsumoto, H., Zhou, Z.B., 2010. Ionic liquids and plastic crystals based on tertiary sulfonium and bis(fluorosulfonyl)imide. Electrochim. Acta 55, 1221–1226.

Hepler, L.G., 1969. Thermal expansion and structure in water and aqueous solutions. Can. J. Chem. 47, 4613–4617.

Hou, X., Zhou, F., Sun, Y., Liu, W., 2007. Ultrasound-assisted synthesis of dentric ZnO nanostructure in ionic liquid. Mater. Lett. 61, 1789.

Jones, G., Dole, M., 1929. 1929, The viscosity of aqueous solutions of strong electrolytes with special reference to barium chloride. J. Am. Chem. Soc. 51, 2950–2964.

Kuhlmann, E., Himmler, S., Giebelhaus, H., Wasserscheid, P., 2007. Imidazolium dialkylphosphates—a class of versatile, halogen-free and hydrolytically stable ionic liquids. Green Chem. 9, 233–242.

Ohno, H., 2006. Functional design of ionic liquids. Bull. Chem. Soc. Jpn. 79, 1665–1680.

Liu, Q., Janssen, M.H.A., van Rantwijk, F., Sheldon, R.A., 2005. Room-temperature ionic liquids that dissolve carbohydrates in high concentrations. Green Chem. 7, 39–42.

MacFarlane, D.R., Forsyth, M., Izgorodina, E.I., Abbott, A.P., Annat, G., Fraser, K., 2009. On the concept of ionicity in ionic liquids. Phys. Chem. Chem. Phys. 11, 4962–4967.

Masson, D.O., 1929. XXVIII. Solute molecular volumes in relation to solvation and ionization. Phil. Mag. J. Sci. 8, 218–235.

Marcus, Y., 1993. Thermodynamics of solvation of ions. Part 6.—the standard partial molar volumes of aqueous ions at 298.15 K. J. Chem. Soc. Faraday Trans. 89, 713–718.

Marcus, Y., 2009. Effect of ions on the structure of water: structure making and breaking. Chem. Rev. 109, 1346–1370.

Matsumoto, H., Sakaebe, H., Tatsumi, K., 2005. Preparation of room temperature ionic liquids based on aliphatic onium cations and asymmetric amide anions and their electrochemical properties as a lithium battery electrolyte. J. Power Sources 146, 45–50.

Moniruzzaman, M., Nakashima, K., Kamiya, N., Goto, M., 2010. Recent advances of enzymatic reactions in ionic liquids. Biochem. Eng. J. 4, 295–314.

Neale, A.R., Murphy, S., Goodrich, P., Hardacre, C., Jacquemin, J., 2017. Thermophysical and electrochemical properties of ethereal functionalised cyclic alkylammonium-based ionic liquids as potential electrolytes for electrochemical applications. ChemPhysChem 18, 2040–2057.

Nie, N., Zheng, D., Dong, L., Li, Y., 2012. 2012, Thermodynamic properties of the water + 1-(2-hydroxylethyl)-3-methylimidazolium chloride system. J. Chem. Eng. Data 57, 3598–3603.

Pernak, J., Czepukowicz, A., Pozniak, R., 2001. New ionic liquids and their antielectrostatic properties. Ind. Eng. Chem. Res. 40, 2379–2383.

Pernak, J., Branicka, M., 2003. The properties of 1-alkoxymethyl-3-hydroxypyridinium and 1-alkoxymethyl-3-dimethylaminopyridinium chlorides. J. Surf. Detergents. 6, 119–123.

Roohi, H., Khyrkhah, S., 2013. Quantum chemical studies on nanostructures of the hydrated methylimidazolium–based ionic liquids. J. Mol. Mod. 21, 1–11.

Schrödinger Release, Desmond Molecular Dynamics System version 4.2, D.E. Shaw Research, New York, NY; 2015. Maestro-Desmond Interoperability Tools, version 4.2, Schrödinger, New York, NY, 2015. 2015.

Schrödinger Release, Jaguar, version 8.8, Schrödinger, LLC, New York, NY, 2015.

Seddon, K.R., 1997. Ionic Liquids for Clean Technology. J. Chem. Technol. Biotechnol. 68, 351–356.

Shekaari, H., Mousavi, S.S., 2009. Conductometric studies of aqueous ionic liquids, 1-alkyl-3-methylimidazolium halide, solutions at T = 298.15–328.15 K. Fluid Phase Equil. 286, 120–126.

Tang, S., Baker, G.A., Zhao, H., 2012. Ether- and alcohol-functionalized task-specific ionic liquids: attractive properties and applications. Chem. Soc. Rev. 41, 4030–4066.

Thomas, D.G., 1965. Transport characteristics of suspension: VIII. A note on the viscosity of Newtonian suspensions of uniform spherical particles. J. Colloid Sci. 20, 267–277.

Tsunashima, K., Sugiya, M., 2007. Physical and electrochemical properties of low-viscosity phosphonium ionic liquids as potential electrolytes. Electrochem. Commun. 9, 2353–2358.

van Rantwijk, Sheldon, R.A., 2007. Biocatalysis in ionic liquids. Chem. Rev. 107, 2757–2785.

Ventura, S.P.M., Sousa, S.G., Serafim, L.S., Lima, A.S., Freire, M.G., Coutinho, J.A.P., 2011. Ionic liquid based aqueous biphasic systems with controlled pH: the ionic liquid cation effect. J. Chem. Eng. Data 56, 4253–4260.

Vraneš, M., Tot, A., Armaković, S., Armaković, S.J., Gadžurić, S., 2016. Structure making properties of 1-(2-hydroxylethyl)-3-methylimidazolium chloride ionic liquid. J. Chem. Thermodyn. 95, 174–179.

Wang, M., Xiao, X., Zhou, X., Li, X., Lin, Y., 2007. Investigation of PEO-imidazole ionic liquid oligomer electrolytes for dye-sensitized solar cells. Sol. Energy Mater. Sol. Cells. 91, 785–790.

Wei, X., Yu, L., Wang, D., Jin, X., Chen, G.Z., 2008. Thermo-solvatochromism of chloro-nickel complexes in 1-hydroxyalkyl-3-methyl-imidazolium cation based ionic liquids. Green Chem. 10, 296–305.

Welton, T., 1999. Room-temperature ionic liquids. solvents for synthesis and catalysis. Chem. Rev. 99, 2071–2084.

Wheatley, R.J., Harvey, A.H., 2007. The water-oxygen dimer: first-principles calculation of an extrapolated potential energy surface and second virial coefficients. J. Chem. Phys. 127, 74303.

Xue, L., Gurung, E., Tamas, G., Koh, Y.P., Maroncelli, M., Quitevis, E.L., 2016. Effect of alkyl chain branching on physicochemical properties of imidazolium-based ionic liquids. J. Chem. Eng. Data 61, 1078–1091.

Yang, Z., Pan, W., 2005. Ionic liquids: Green solvents for nonaqueous biocatalysis. Enzyme Microbial. Technol. 37, 19–28.

Yokozeki, A., Shiflett, M.B., 2010. Water solubility in ionic liquids and application to absorption cycles. Ind. Eng. Chem. Res. 49, 9496–9503.

Yoshizawa, M., Ohno, H., 2001. Synthesis of molten salt-type polymer brush and effect of brush structure on the ionic conductivity. Electrochim. Acta. 46, 1723–1728.

Yue, C., Fang, D., Liu, L., Yi, T.F., 2011. Synthesis and application of task-specific ionic liquids used as catalysts and/or solvents in organic unit reactions. J. Mol. Liq. 163, 99–121.

Zhang, S., Qi, X., Ma, X., Lua, L., Zhang, Q., Deng, Y., 2012. Investigation of cation–anion interaction in 1-(2-hydroxyethyl)-3-methylimidazolium-based ion pairs by density functional theory calculations and experiments. J. Phys. Org. Chem. 25, 248–257.

Zhao, H., 2010. Methods for stabilizing and activating enzymes in ionic liquids—a review. J. Chem. Tech. Biotechnol. 85, 891–907.

Zhou, Z.B., Matsumoto, H., Tatsumi, K., 2006. Cyclic quaternary ammonium ionic liquids with perfluoroalkyltrifluoroborates: synthesis, characterization, and properties. Chem. Eur. J. 12, 2196–2212.